

Bulletin of the Seismological Society of America

This copy is for distribution only by
the authors of the article and their institutions
in accordance with the Open Access Policy of the
Seismological Society of America.

For more information see the publications section
of the SSA website at www.seismosoc.org



THE SEISMOLOGICAL SOCIETY OF AMERICA
400 Evelyn Ave., Suite 201
Albany, CA 94706-1375
(510) 525-5474; FAX (510) 525-7204
www.seismosoc.org

The Use of Spectral Content to Improve Earthquake Early Warning Systems in Central Asia: Case Study of Bishkek, Kyrgyzstan

by Jacek Stankiewicz, Dino Bindi, Adrien Oth, Massimiliano Pittore, and Stefano Parolai

Abstract Expansion of urban areas in Central Asia increases their exposure to seismic hazard, but at present no earthquake early warning (EEW) systems exist in the region. Such systems, successfully implemented in other regions, aim to provide warning of the order of tens of seconds about impending disasters, enabling the first rapid-response steps to be taken. The feasibility of such systems for Bishkek, Kyrgyzstan, has been demonstrated. This study investigates how the use of the spectral content, instead of just ground-motion thresholds, can be used to improve the performance of proposed regional warning systems. We find that using the spectral content of the first few seconds after the *P*-wave arrival can provide timely warning for events closer to the target city than was possible with the threshold systems. It is further shown that for events less than 60 km from the target, any regional system needs to be complemented with an onsite one to provide a comprehensive EEW system.

Introduction

The proximity of many large cities (e.g., Tokyo, Istanbul) to seismically active zones, and the resulting earthquake risk, has led to the development of earthquake early warning (EEW) systems. Such systems aim to provide a warning to the city after an earthquake has occurred but before the potentially destructive seismic waves arrive (Satriano *et al.*, 2011, and references therein). In this time, typically in the order of seconds to tens of seconds, several damage-control and mitigation steps can be taken, such as orderly suspension of activities in hospitals or shut downs of power supplies (Allen *et al.*, 2009; Nakamura *et al.*, 2011).

Various types of EEW systems have been proposed and developed (see Satriano *et al.*, 2011, for a review). Broadly speaking, two types of systems exist. Regional systems use a network of stations, typically deployed between the seismogenic zone and the target city, and attempt to provide timely information about the expected ground motion. The alternative approach, onsite systems, involves one or more sensors placed at the target, with the aim of detecting the early coda of the earthquake (typically the *P* wave) and issuing a warning regarding the impending arrival of more damaging waves (typically the *S* and surface waves). Additionally, regional systems generally provide the location and magnitude of the event, whereas onsite systems typically work with ground-motion thresholds being exceeded. Regional systems take advantage of electronically transmitted information traveling faster than the destructive seismic waves. The recorded signal can thus be transmitted and analyzed, and a warning issued, before the most damaging waves reach the city or target concerned. The key parameter in all EEW systems is the lead time, which is typically considered as the time between the warning

being issued and the arrival of the destructive seismic wave-trains. The exact definition of this time, however, varies among different systems, and will be discussed further in this article.

Central Asia faces significant earthquake hazard and risk. In particular, rapid urbanization of major cities in the region, such as Bishkek and Almaty (Fig. 1), makes the population vulnerable to such natural hazards (e.g., Abdrakhmatov *et al.*, 2003; Bindi *et al.*, 2011; Wieland *et al.*, 2015). Despite this exposure, no earthquake warning systems currently exist in the region. The capital city of Kyrgyzstan has previously been used as a case study to demonstrate the necessity and feasibility of using networks of stations for such systems in the region (Picozzi *et al.*, 2013; Pittore *et al.*, 2014). The study presented here builds on those efforts, presenting a new, efficient type of regional warning systems and demonstrating how they can be incorporated into a modern earthquake warning–rapid response system.

Ground Acceleration Based Systems and Optimization

One important aspect in developing a regional EEW system is the network geometry. Zollo *et al.* (2009) first performed network evaluations and showed how improvements can be made. Oth *et al.* (2010) developed a technique for designing optimal EEW systems, using an acceleration threshold based methodology as an example. The main attractiveness of this methodology lies in its simplicity, and its applicability to Central Asia has since been demonstrated (Stankiewicz *et al.*, 2013; Pittore *et al.*, 2014). The method

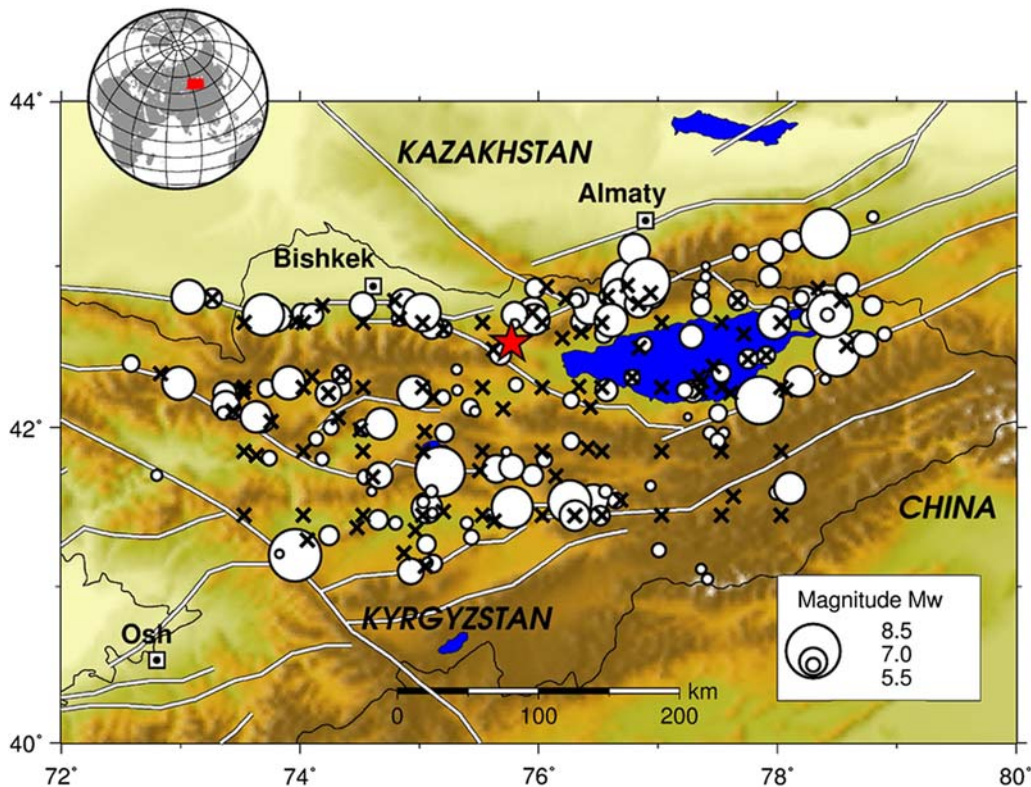


Figure 1. The study area, showing major active tectonic features (white lines). The 150 scenario dataset earthquake is marked as circles, and the source dataset as crosses. Event used for calibration (Fig. 2) marked with a star. See text for further explanation. The color version of this figure is available only in the electronic edition.

considers a number of potential station locations and a set of scenario events representative of the seismic hazard facing the target city. These scenarios are generated by defining moment magnitude, stress parameter, and fault mechanism. Oth *et al.* (2010) used 128 station locations and 180 events for the case study of Istanbul, which was used as an example case to illustrate the approach.

For each station location–scenario event pair, synthetic ground acceleration traces are computed, using the finite-source ground-motion simulation code EXSIM (Motazedian and Atkinson, 2005; Boore, 2009). This is a stochastic finite-fault simulation code where simplified models are used to describe source, path, and site effects. This approach is ideally suited for the purposes of our study, as our emphasis is not on the simulation of the complete wavefield for given scenario earthquakes, but rather on the generation of a large set of spectra for hypothetical sources located according to a seismic catalog. The program divides a large fault into a set of subfaults, treating each of them as a point source. The ground motion at given points resulting from the entire fault is then the sum of contributions of the subfaults, each of which is calculated by the stochastic point source method. Synthetic traces for all scenarios at the target city were also calculated, specifically at 19 station locations installed in Bishkek for the purpose of studying site effects (Ullah *et al.*, 2013). To quantify the accuracy of warnings, all scenario events must be assigned the expected warning class for the

target. Previous studies (Oth *et al.*, 2010; Stankiewicz *et al.*, 2013) based these warning classes on the peak ground acceleration generated at the target. Here, seismic intensity expected in Bishkek is considered as a more appropriate parameter, with the technique of Sokolov and Chernov (1998) used to estimate it. Four expected warning classes were considered. When the seismic intensity does not reach IV at any of the 19 sites, no warning is deemed necessary, and the event is classified as class 0. Classes I, II, and III are then defined when the intensity reaches at least IV, VI, and VII, respectively. The first class, associated with intensity IV, refers to an event “largely observable” (see Grünthal *et al.*, 1998, for all references to European Macroseismic Scale [EMS]-98 intensity and vulnerability classes hereafter). Even though no damage is expected, such an event should be accompanied by suitable public communication from the civil protection authorities to prevent unmotivated panic among the exposed population. The second class is triggered by intensity VI, which is usually associated with the occurrence of damage in the most vulnerable buildings (the action previously mentioned always applies from class I onward). Events of class II could require emergency protocols focusing on the alerting of critical services such as fire brigades and police corps. Class III refers to a potentially damaging earthquake, because intensity VII is generally associated with extensive structural damage of the highly vulnerable structures (vulnerability classes A and B according to EMS-98 scale) and implies the possibility of casualties. This warning class could

thus trigger more incisive mitigation actions including the controlled interruption of gas and oil pipelines, and the deployment of emergency response units (more details about the possible response measures can be found, e.g., Lee and Espinosa-Aranda, 2002; Nakamura *et al.*, 2011).

For any hypothetical network, a so-called cost can be computed for each scenario event, using the accuracy of the warning and the available warning time. This cost value provides an objective criterion for evaluating the EEW performance of the hypothetical network for a given scenario event. The network is defined by the locations of a predefined number of stations (for instance 10, following Stankiewicz *et al.*, 2013), and three ground acceleration threshold values. These values are the same for all stations and represent the three non-zero warning classes. As soon as one of the network threshold levels is exceeded at any three stations in a time window of 5 s, the corresponding warning level is issued at the target. The warning time is defined as the time between this warning (i.e., the third station being triggered) and the *S*-wave reaching the target. An important question is what constitutes a sufficient warning time, the algorithms used in this study aim to provide a warning of 10 s. Given the proximity of Bishkek to active seismogenic zones, with a number of considered scenarios closer than 100 km, no regional system will be able to provide a 10 s warning for these events. For this reason, any regional system proposed in this study will need to be complemented by an onsite system, such as the one outlined by Bindi *et al.* (2015).

For each scenario, the accuracy of the warning is a simple binary function: was the correct warning class issued? If not, the scenario cost is assigned a value of 1, which is the maximum scenario cost. If the correct class was identified, the cost approaches 0 (the minimum allowed) for large lead times, is 0.5 at 10 s, and tends to 1 because the time decreases toward 0. The cost of the network is then computed as a weighted average of individual scenario costs (see Oth *et al.*, 2010, for details on the cost function definition). Using such a cost function, it is possible to search for optimal network designs (station locations and trigger thresholds). For solving this nonlinear optimization problem, genetic algorithms are used (see Oth *et al.*, 2010, for more details).

Spectral Systems

As mentioned earlier, the attractiveness of such acceleration threshold based systems lies in their simplicity and ease to implement. However, the only information used is the ground-motion amplitude, and the waveforms recorded by the EEW system clearly contain more information that can be exploited to increase its efficiency and robustness. Indeed, systems utilizing spectral parameters have been applied for regions such as Japan and California (Wu *et al.*, 2007; Shieh *et al.*, 2008). The concept we propose in this article is to compute the spectrum of the first few seconds after an event has been detected, and to compare this with a precomputed spectral library associated with the recording station. Constructing such a library from available observational data alone is even

difficult (if not impossible) in densely instrumented regions such as California or Japan, let alone in Kyrgyzstan. In the same way, resorting to observational data alone will never allow for a consideration of a representative set of potentially relevant scenarios. Finally, while in principle observations from weak motion instruments would be sufficient to calculate the spectra of the early *P* wave without clipping in most cases, strong-motion records are indispensable to link these spectra with a prediction of ground shaking at the target, as we do in this work. For these reasons, we resort to stochastic simulations to construct the spectral library and optimize/test the proposed system's performance.

For the training phase of the algorithm, a source dataset representative of the seismic hazard in the area is required. Of the 100 event locations considered, 60 were randomly distributed along tectonic faults in the study area and 40 were placed on a regular grid spanning the area. For each location, 17 possible moment magnitudes (from 4 to 8 in steps of 0.25), 4 stress parameter values (10, 25, 50, and 75 MPa), and 3 dip values for the fault (30°, 45°, and 60°) were used. The strike of the fault was fixed, for the locations along faults the orientation of the relevant fault segment was used, and for the 40 grid locations the orientation of the nearest fault with a random adjustment did not exceed 10°. All faults were assumed to be reverse faults, consistent with the dominant fault mechanism in the region. This resulted in 204 possible events for each location.

For prospective station locations, 256 were considered, spaced on a 0.2° grid between 41.6° and 43° N and 72.8° and 79° E. EXSIM was used to simulate ground motion for each event at each of these locations, as well as at 19 station locations installed in Bishkek for the purpose of studying site effects (Ullah *et al.*, 2013). A rate of 100 samples per second was used for all synthetic traces. *P* and *S* waves were computed separately (as in Böse, 2006), resulting in over 10 million traces. The *P* and *S* traces were added together using the appropriate time shift to obtain complete traces for each station–event pair. Seismic velocity models and most other EXSIM parameters were set to similar values as used by Picozzi *et al.* (2013) and Stankiewicz *et al.* (2013). Anelastic attenuation was assumed, with *Q* factors being frequency dependent: 570 for frequencies under 1.4 Hz, and scaled with $f^{0.7}$ for higher frequencies. This was for *P* waves, following Böse (2006), a Q_P/Q_S ratio of 9/4 was assumed. The suitability of the input parameters was confirmed by comparison of synthetic traces with those recorded on the vertical component of the accelerometer of the vertical array in Bishkek (Parolai *et al.*, 2013). Site amplification effects were estimated from the topographic slope, which can be considered a proxy for shear-wave velocity of the uppermost 30 m, V_{S30} (Wald and Allen, 2007). An example comparing real recorded data to the synthetic traces is shown in Figure 2. The recording of a magnitude 5.1 event 90 km from Bishkek was used, and synthetic traces were generated using these parameters. Stress drop and fault dip were varied as listed above, resulting in 12 permutations. As an example, the trace with

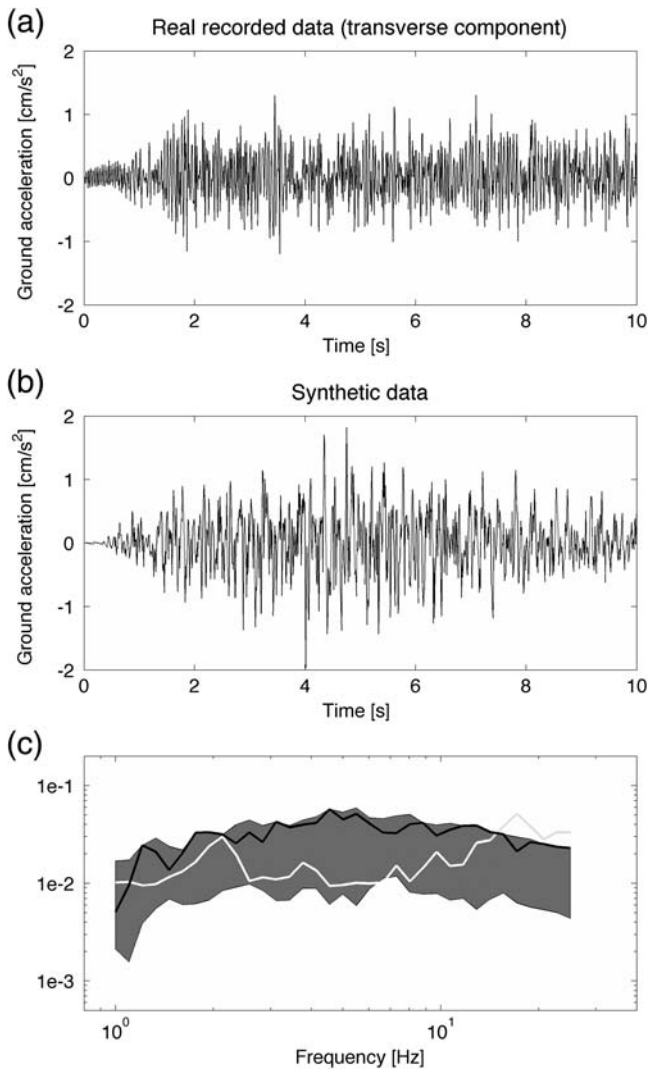


Figure 2. Validation of EXSIM parameters with real data. (a) Recording (transverse component) of an M_w 5.1 event 90 km from Bishkek on 23 November 2013 (see Fig. 1 for location). (b) Example of an EXSIM simulation using the same magnitude and epicentral distance. (c) Comparison of the spectra smoothed as described in the text. Envelope of the 12 synthetic spectra is shaded in gray, with the spectrum of the example trace from (b) in black. The spectrum of the recorded trace in white.

a stress drop of 75 MPa and a dip angle of 45 is shown, and all 12 spectra are incorporated into Figure 2. The spectra were smoothed using the algorithm of Konno and Ohmachi (1998), using 35 frequency values spaced logarithmically between 1 and 25 Hz.

Once the synthetic traces had been computed, we used this large-scale simulation dataset to generate a spectral library to be used within the proposed early warning methodology. At all prospective station locations, power spectra of the first 5, 7, and 9 s since the P -wave onset were computed for all traces. To make sure no energy from the onset is lost, the time windows were started 0.5 s before the onset. The spectra were smoothed using the algorithm of Konno and Ohmachi (1998), using the same parameters as for the validation traces dis-

cussed above. The spectral library thus consists of 20,400 smoothed spectra for each of the three time window lengths at each of 256 prospective station locations. In turn, the traces computed for the locations at the 19 Bishkek stations (Ullah *et al.*, 2013) were used to estimate the seismic intensity resulting from each set of source parameters. To this end, the technique of Sokolov and Chernov (1998) was again used to provide seismic intensity estimates for the different parts of the Kyrgyz capital. In summary, the system aims to compare the power spectra of a recorded event that triggered the system to the spectra stored in the library. For each of the scenarios in the library, the seismic intensity information for Bishkek has also been calculated, so the ground shaking severity at the target can be rapidly estimated once the most likely scenario event has been selected.

A clear advantage of this kind of warning system is that intensity estimates at the target can be attempted as soon as any single-station registers an arrival. Although using just one station is likely to cause significant uncertainties due to evident ambiguities in the best scenario event selection from the spectral library, more accurate intensity estimates, and thus warnings, can be provided as more stations register the event. Once any n stations in the network have recorded at least 5 s of signal, the spectra are computed and smoothed using the same parameters as were used to generate the library. If the earlier stations have recorded 7 or 9 s since the trigger by the time the n th station recorded 5 s, the longer windows are used. At each of the stations the L1 norm is used to calculate the misfit between the observed signal and each spectrum in the library. The misfits are then added for all stations, with the best scenario selected. The seismic intensity associated with this scenario is the intensity estimate used for the warning to the target city. These warnings can be issued in an evolutionary way, with an updated warning every time a new station triggers upon the event.

To evaluate the performance of any proposed network and find the optimal network geometry, a scenario dataset is of course necessary. This dataset should be independent of the source dataset constituting the basis of the spectral library, though because both datasets need to be the representative of the real earthquakes likely to occur, some overlap between them is unavoidable. To this end, 150 events were defined, varying in magnitude between 4.1 and 8.4, and in stress value between 21 and 85 MPa, were chosen (Fig. 1). These events comprise historical events, locations along active tectonic faults, as well as random events. Although it is impossible to consider every scenario, this selection is considered appropriate for presenting the concept of spectral systems. The systems this study presents are optimized for the known seismic hazard for Bishkek, as represented by this portfolio. It should be noted that although some active tectonic faults exist north of Bishkek (Fig. 1), no event with magnitude 5 or larger has been observed there in historical catalogs (Mikhailova *et al.*, 2015), and thus no scenarios were considered in that zone. The 150 events were identical to the ones used by Pittore *et al.* (2014) for incorporating

Table 1

Performance of the Optimal Network for Each System Type

System Used	Cost	% Correct Warning	Mean Lead Time (s)
Acceleration	0.482	84	13.4
Spectral, 1 station	0.452	73	28.1
Spectral, 2 stations	0.405	75	20.2
Spectral, 3 stations	0.404	80	18.4
Spectral, 4 stations	0.388	84	16.0
Spectral, 5 stations	0.448	83	14.0

threshold-based warning systems into a rapid response system for Bishkek. Furthermore, the 256 potential station locations are also the same. This enables direct comparisons between the threshold-based and spectral-based EEW methodologies, and keeps the work presented here in the framework of ongoing Central Asia projects.

To assess whether the proposed spectral-based system design will provide an advance over the simpler threshold-based approach, we compare the performance of the best system designs found through genetic algorithm optimization runs in both cases. However, care needs to be taken to ensure that the optimization results for the design of EEW systems based on the two different approaches are actually comparable. The cost function definition of any network using spectral data analysis must be similar to the threshold-based one, so that the optimization runs are carried out relative to the same (or at least reasonably similar) objective criteria. In contrast to the threshold-based approach where the optimal network thresholds need to be determined in addition to the best station locations, the optimal spectral system only requires the definition of the station locations. In the spectral system case, the lead time is defined as the time between the warning being issued (5 s after the 3rd station records the *P*-wave onset) and the potentially destructive *S*-wave reaching Bishkek. To quantify the accuracy of the warning and allow for a direct comparison with the threshold-based approach, warning classes are defined as before, based on the seismic intensity values in Bishkek reaching at least IV, VI, and VII, with the warning accuracy again a binary function. The cost of the network is then a function of lead time and accuracy, similar to what was used for the threshold-based systems, with the only difference being the definition of the lead time.

Results and Discussion

Genetic algorithms were run 10 times for the threshold-based system design. This was necessary due to the randomness present in the algorithm. For the spectral system case, four cases were considered, depending on how many (1–4) stations are required to record at least 5 s of signal for the cost function to be computed. For each case independent trials were performed. Networks of 10 stations were considered throughout, and to enable direct comparisons, the expected warning classes were defined in an identical manner using intensity values for Bishkek for all cases. With the classes thus

defined, of the 150 scenario events 77 were class 0 events for which no warning is necessary and 56, 9, and 8 events were in the warning classes I, II, and III, respectively.

After each algorithm converged successfully, not only the system design with the lowest cost function, but also those with slightly higher cost values were all retained. The result of this is a collection of over 1000 efficient EEW network configurations. This is important for the end users, such as authorities in Bishkek, because it enables further constraints to be placed on selecting an EEW system configuration. These constraints could include limited access to a particular location for station deployment or maintenance, or the availability of wireless communication.

For each type of system, the performance of the system with the lowest cost function computed is shown in Table 1. In addition to the cost function, the percentage of correctly classified events and the mean lead time are also given. From the table it is clear that the most efficient systems are the spectral ones, which utilize recordings from four stations, though reliable warnings can be issued with spectral systems utilizing just three, or even two, stations. Although their accuracy is similar to the acceleration-based systems, which use three stations, the spectral systems provide larger lead times. The reason for this is that the spectral systems begin operation at the *P*-wave arrivals, whereas acceleration thresholds are typically first exceeded by the *S* waves that arrive later. Another result is that the accuracy of warnings does not increase if the spectral system waits for a fifth station to record a signal. This results in increasing the cost function, because the lead time is decreased while the system waits for the additional trigger. The geometry and performance of the best spectral system, optimized for four station triggers, is shown in Figure 3. It is particularly worth noting that all large (class II and III) events would be detected, though a small portion of them would be misclassified.

Because it is nearly impossible to present all the EEW network designs computed here, we present the station locations most commonly appearing in the solutions, thus likely to represent strategic locations for a functional system. Figure 4a shows the location of the stations appearing in at least 10% of the best 1000 spectral systems. The stations are marked according to how frequently they feature in the solutions. The corresponding station distribution for the threshold-based systems is shown in Figure 4b.

From Figure 4a,b, it is apparent that the two different approaches produce completely different network geometries. The threshold-based systems rarely have a station within 100 km of Bishkek, which results in a significant blind zone, where any event within that distance of the city will effectively be ignored as long as a warning time of 10 s is considered desirable. Conversely, various locations close to Bishkek are utilized by the spectral systems. Although the blind zone has not been eliminated, its size is now approximately 60 km (Fig. 3c, right). This can be reduced further by defining the cost function to be more tolerant of warning times between 5 and 10 s (Stankiewicz *et al.*, 2013). However, the zone cannot be eliminated altogether, and a complete EEW

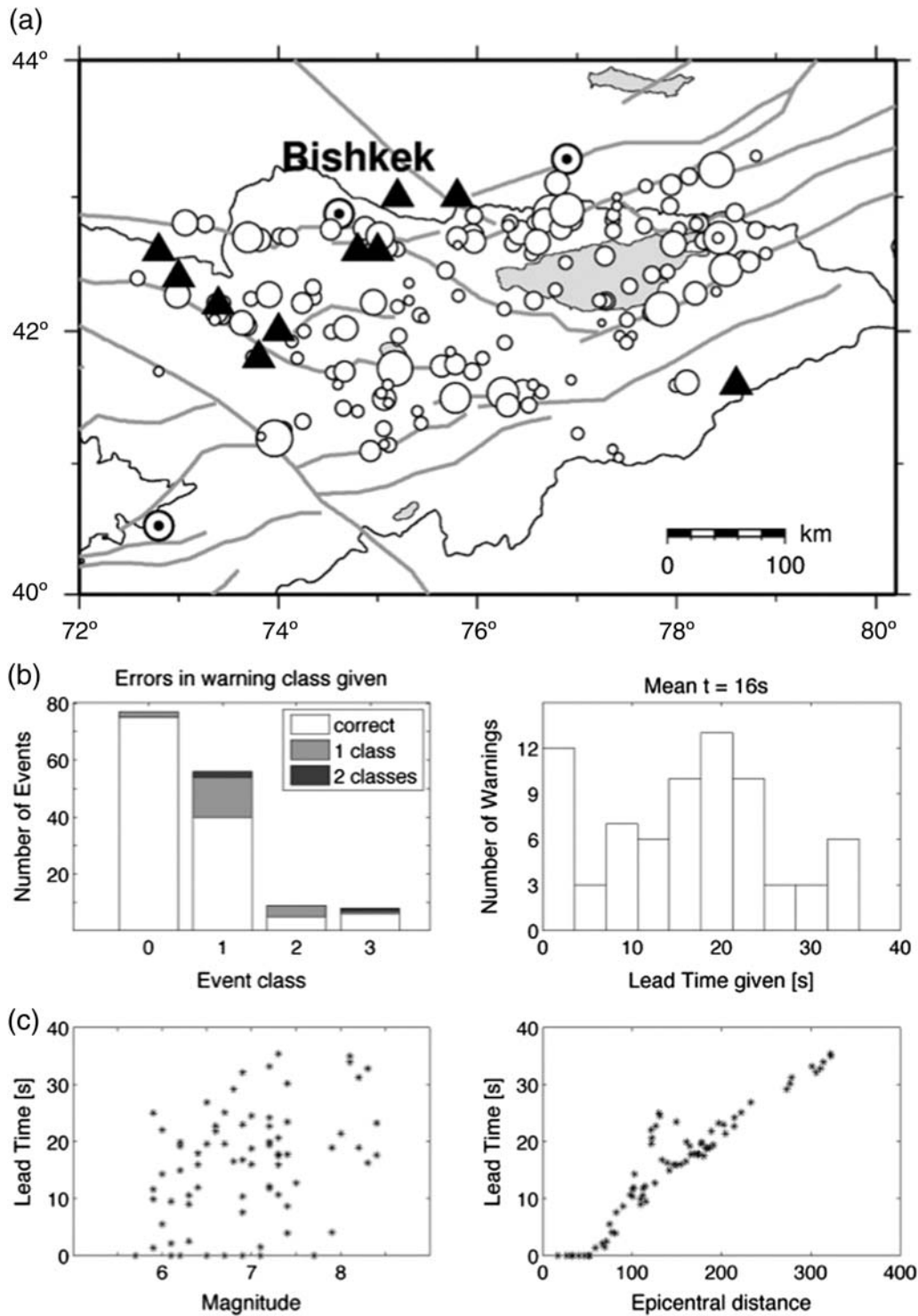


Figure 3. The most efficient network computed in the study. (a) The station distribution (black triangles) with the 150 events and the outline of Kyrgyzstan in the background. (b) (left) Accuracy (and level of misclassification) of estimating the warning class. (right) Histogram of warning times. (c) Distribution of warning times as functions of magnitude and epicentral distance.

system should incorporate an onsite system alongside a regional system presented here. The ability of spectral systems to issue warnings for the events between 60 and 100 km from Bishkek is likely to be one of the reasons for their superior performance. It is also clear that much fewer stations dominate

the best solutions of the spectral systems, no station appeared in over 30% of the best 1000 solutions, and just six stations featured in 15%. This implies there are fewer, if any, critical locations for spectral systems, which gives more freedom to considering logistics of installing a network.

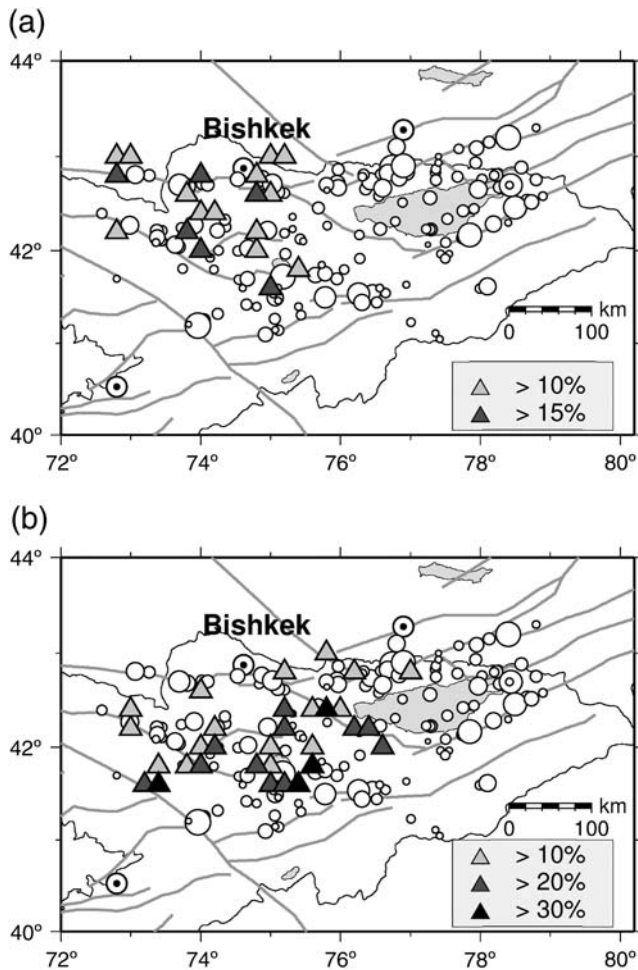


Figure 4. Stations appearing in at least 10% of the best 1000 solutions of the (a) spectral and (b) threshold-based systems.

An important advantage of spectral systems is that they can issue warnings in an evolutionary way, as soon as a single station has detected an event. As more data become available, even a system optimized for three triggers, preliminary warnings could be issued using data recorded by one and two stations. These warnings could then be updated as more data are recorded. As an example, a magnitude 7.5 scenario event 120 km from Bishkek is shown in Figure 5. This would reach intensity VI in Bishkek, and thus be a class II event. Using the network from Figure 3, the nearest station would have a 5 s recording 10 s before the *P* wave reaches Bishkek. Processing this 5 s signal would classify the event as a class I, and a warning, albeit for a wrong class, would be issued. Two seconds later, 5 s of recording at a second station, combined with 7 s available at the first, would classify the event as class II, and warning could be updated. The warning would be confirmed another 5 s later, with the third station available, and the first two having 9 s each. The last confirmation, with four stations processed, would arrive between the *P* and *S* waves, though some action should already have been taken by then.

Besides the simple comparisons to real data (Fig. 2), the entire process behind the system proposed in this study relies

on synthetic seismograms. This is largely the result of sparse strong-motion data recordings in Central Asia. To test whether the proposed system of matching spectra to a synthetic library is viable for real data, we use the well-recorded M_w 6.8 Niigata event from Japan. The event was recorded by 114 stations of the K-NET and KiK-net networks (Oth *et al.*, 2011). In this validation, we replace the scenario from Figure 5 with the Niigata event, and provide the four nearest stations with traces recorded at the matching offsets. The spectra of these traces (9 s of signal for the three nearest stations, 5 s for the fourth station) were then compared with the synthetic spectral libraries using the approach presented earlier (Fig. 6). The best fit corresponded to a scenario just east of where the event was placed, as was the case for the synthetic test presented in Figure 5. The magnitude was estimated as 7. This difference is less than the increment used in our simulations (0.25), and thus we consider the fit sufficiently good to confirm the viability of the approach presented here.

Conclusions

In this article, we present a new technique for designing efficient regional EEW systems, using the city of Bishkek as a case study. The new technique uses the entire waveform of the first few seconds of arriving signal. By modifying existing methods for quantifying the system performance, genetic algorithms are used to find the most efficient network geometries, and it is shown that the new systems are an improvement on systems only using signal amplitude as input. Significantly, the geometries of efficient networks using the spectrum of the full waveform are found to be different to those dealing with just the signal amplitude. Thus prior to the deployment, it is important to use an objective assessment approach to decide on the system type to be deployed, as changing that after the installation is likely to render the network inefficient.

Although only the most efficient EEW network identified in this study has been illustrated, it is important to stress that hundreds of network configurations capable of similar performance have been identified. This allows further selection criteria to be applied to the results before a network is installed, such as particular locations becoming inaccessible.

It must also be stressed that the systems are optimized for the seismic hazard for Bishkek, as represented by the event portfolio. With better understanding of the hazard in the framework of ongoing studies (e.g., Bindi *et al.*, 2015; Ullah *et al.*, 2015), the optimizations would need to be performed again using the concepts developed in this study.

Last, it needs to be noted that the balance between the timing and accuracy of a warning is very delicate. Although a network needs to be assigned a single cost value for computational purposes, no system can be installed with just this single figure in mind. The networks presented here are just a step in the complex earthquake rapid response system (Pittore *et al.*, 2014), and their individual performance needs to

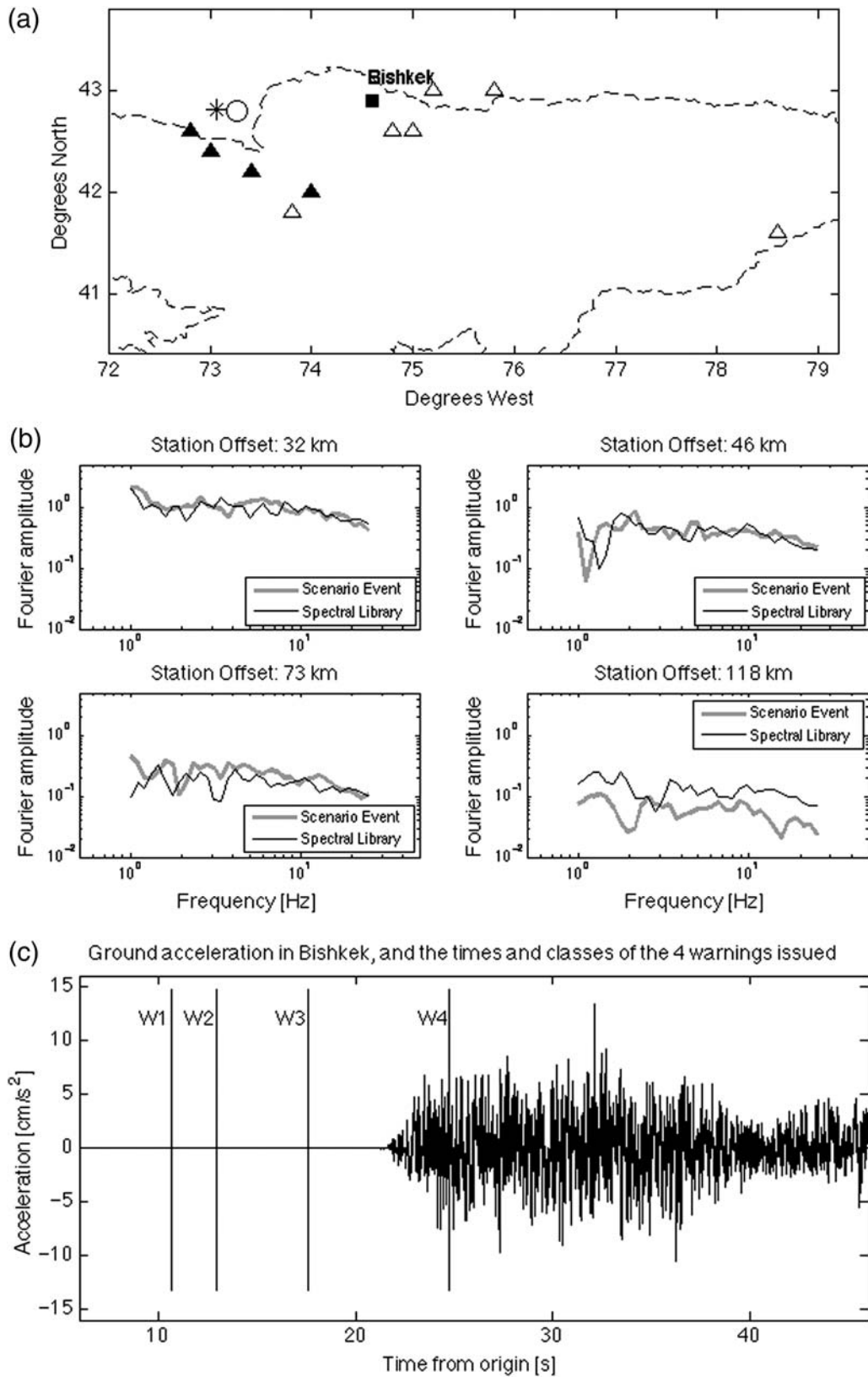


Figure 5. Example of how the system shown in Figure 3 functions for a single class II scenario event. (a) The considered scenario (star) and the station locations as triangles, with the four nearest to the epicenter in black. The location of the event chosen from the library as the best fit is marked with a circle. (b) Smoothed spectra of the scenario signal and the best-fit event chosen from the precomputed library. (c) The acceleration trace (in cm²/s²) recorded in Bishkek, and times and classes of warnings issued. Once data from two stations are processed, the correct class II warning would be issued, and confirmed once the third and fourth station data have been processed.

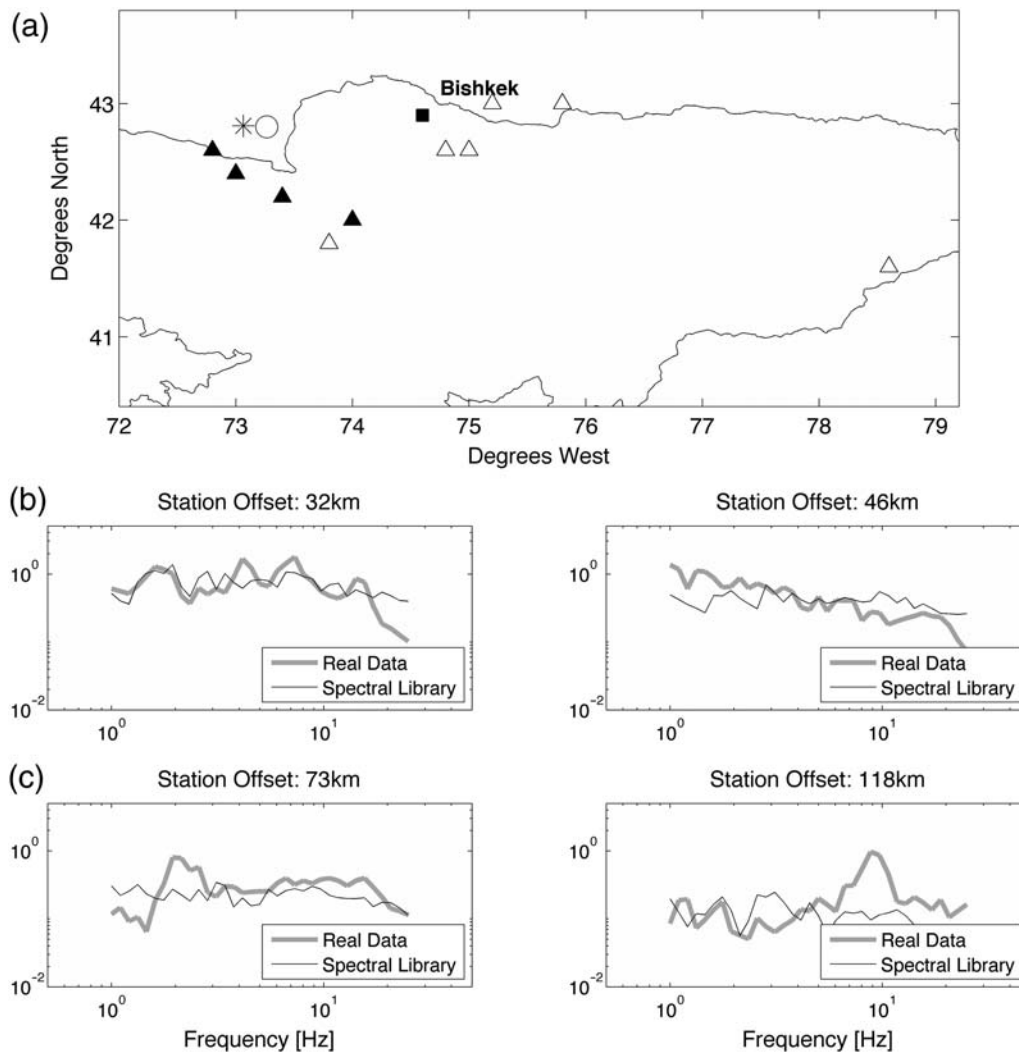


Figure 6. Testing the system with real data from the M_w 6.8 Niigata earthquake in Japan. (a) The scenario (star) from Figure 5 was replaced by real data recorded at offsets corresponding to those to the nearest four stations (marked in black). (b,c) The spectral fits are not as good as for synthetic data, but the event is relocated with the same previous accuracy. The magnitude is estimated as M_w 7.

be carefully evaluated by scientists, installation and maintenance teams, and the authorities in Bishkek.

Data and Resources

The data recorded in Kyrgyzstan used to calibrate the parameters for synthetic traces are available on the Geofon network (geofon.gfz-potsdam.de). The K-NET and KiK-net data can be found at www.kik.bosai.go.jp. All these websites were last accessed for the purposes of this study in January 2015.

Acknowledgments

The research is funded by the Fonds National de la Recherche, Luxembourg, cofunded by the Marie Curie Actions of the European Commission (FP7-COFUND) (AFR project 4817114), with support from the Advanced Remote Sensing-Ground Truth Demo and Test Facilities (ACROSS) initiative of the Helmholtz Association. Constructive criticism from two anonymous reviewers significantly improved the manuscript.

References

- Abdrakhmatov, K., H.-B. Havenith, D. Delvaux, D. Jongmans, and P. Trefois (2003). Probabilistic PGA and arias intensity maps of Kyrgyzstan (Central Asia), *J. Seismol.* **7**, 203–220.
- Allen, R. M., P. Gasparini, O. Kamigaichi, and M. Böse (2009). The status of earthquake warning around the world: An introductory overview, *Seismol. Res. Lett.* **80**, no. 5, 682–693.
- Bindi, D., T. Boxberger, S. Orunbaev, M. Pilz, J. Stankiewicz, M. Pittore, I. Iervolino, E. Ellguth, and S. Parolai (2015). On-site early-warning system for Bishkek (Kyrgyzstan), *Ann. Geophys.* **58**, S0112, doi: [10.4401/ag-6664](https://doi.org/10.4401/ag-6664).
- Bindi, D., M. Mayfield, S. Parolai, S. Tyagunov, U. T. Begaliev, and K. Abdrakhmatov (2011). Towards an improved seismic risk scenario for Bishkek, Kyrgyz Republic, *Soil Dyn. Earthq. Eng.* **31**, 521–525.
- Boore, D. M. (2009). Comparing stochastic point-source and finite-source ground-motion simulations: SMSIM and EXSIM, *Bull. Seismol. Soc. Am.* **99**, no. 6, 3202–3216.
- Böse, M. (2006). Earthquake early warning for Istanbul using artificial neural networks, *Ph.D. thesis*, University of Karlsruhe, Germany.
- Grünthal, G., and European Seismological Commission (1998). European macroseismic scale 1998: EMS-98: Luxembourg, European

- Seismological Commission Subcommittee on Engineering Seismology Working Group Macroseismic scales.
- Konno, K., and T. Ohmachi (1998). Ground-motion characteristics estimated from spectral ratios between horizontal and vertical components of microtremors, *Bull. Seismol. Soc. Am.* **88**, 228–241.
- Lee, W. H. K., and J. M. Espinosa-Aranda (2002). Earthquake early warning systems: Current status and perspectives, in *Early Warning Systems for Natural Disaster Reduction*, J. Tschau and A. N. Küppers (Editors), Springer-Verlag, Berlin, Germany, 409–423.
- Mikhailova, N. N., A. S. Mukambayev, I. L. Aristova, G. Kulikova, S. Ullah, M. Pilz, and D. Bindi (2015). Central Asia earthquake catalogue from ancient time to 2009, *Ann. Geophys.* **58**, S0102, doi: [10.4401/ag-6681](https://doi.org/10.4401/ag-6681).
- Motazedian, D., and G. M. Atkinson (2005). Stochastic finite-fault modeling based on a dynamic corner frequency, *Bull. Seismol. Soc. Am.* **95**, 995–1010.
- Nakamura, Y., J. Saita, and T. Sato (2011). On an earthquake early warning system (EEW) and its applications, *Soil Dyn. Earthq. Eng.* **31**, 127–136.
- Oth, A., M. Böse, F. Wenzel, N. Köhler, and M. Erdik (2010). Evaluation and optimization of seismic networks and algorithms for earthquake early warning—the case of Istanbul (Turkey), *J. Geophys. Res.* **115**, no. B10311, doi: [10.1029/2010JB007447](https://doi.org/10.1029/2010JB007447).
- Oth, A., S. Parolai, and D. Bindi (2011). Spectral analysis of K-NET and KiK-net data in Japan, Part I: Database compilation and peculiarities, *Bull. Seismol. Soc. Am.* **101**, no. 2, 652–666.
- Parolai, S., D. Bindi, S. Ullah, S. Orunbaev, S. Usupaev, B. Moldobekov, and H. Echter (2013). The Bishkek vertical array (BIVA): Acquiring strong motion data in Kyrgyzstan and first results, *J. Seismol.* **17**, 707–719.
- Picozzi, M., D. Bindi, M. Pittore, K. Kieling, and S. Parolai (2013). Real-time risk assessment in seismic early warning and rapid response: A feasibility study in Bishkek (Kyrgyzstan), *J. Seismol.* **17**, 485–505.
- Pittore, M., D. Bindi, J. Stankiewicz, A. Oth, M. Wieland, T. Boxberger, and S. Parolai (2014). Towards a loss-driven earthquake early warning and rapid response system for Kyrgyzstan (Central Asia), *Seismol. Res. Lett.* **85**, no. 6, 1328–1340.
- Satriano, C., Y.-M. Wu, A. Zollo, and H. Kanamori (2011). Earthquake early warning: Concepts, methods and physical grounds, *Soil Dyn. Earthq. Eng.* **31**, 106–118.
- Shieh, J.-T., Y.-M. Wu, and R. M. Allen (2008). A comparison of τ_c and τ_p^{\max} for magnitude estimation in earthquake early warning, *Geophys. Res. Lett.* **35**, L20301, doi: [10.1029/2008GL035611](https://doi.org/10.1029/2008GL035611).
- Sokolov, V. Y., and Y. K. Chernov (1998). On the correlation of seismic intensity with Fourier amplitude spectra, *Earthq. Spectra* **14**, no. 4, 679–694.
- Stankiewicz, J., D. Bindi, A. Oth, and S. Parolai (2013). Designing efficient earthquake early warning systems: Case study of Almaty, Kazakhstan, *J. Seismol.* **17**, 1125–1137.
- Ullah, S., D. Bindi, M. Pilz, and S. Parolai (2015). Probabilistic seismic hazard assessment of Bishkek, Kyrgyzstan, considering empirically estimated site effects, *Ann. Geophys.* **58**, S0105, doi: [10.4401/ag-6682](https://doi.org/10.4401/ag-6682).
- Ullah, S., D. Bindi, M. Pittore, M. Pilz, S. Orunbaev, B. Moldobekov, and S. Parolai (2013). Improving the spatial resolution of ground motion variability using earthquake and seismic noise data: The example of Bishkek (Kyrgyzstan), *Bull. Earthq. Eng.* **11**, 385–399.
- Wald, D. J., and T. I. Allen (2007). Topographic slope as a proxy for seismic site conditions and amplification, *Bull. Seismol. Soc. Am.* **97**, 1379–1395.
- Wieland, M., M. Pittore, S. Parolai, U. Begaliev, P. Yasunov, J. Niyazov, S. Tyagunov, B. Moldobekov, S. Saidiy, I. Ilyasov, and T. Abakanov (2015). Towards a cross-border exposure model for the Earthquake Model Central Asia, *Ann. Geophys.* **58**, S0106, doi: [10.4401/ag-6663](https://doi.org/10.4401/ag-6663).
- Wu, Y.-M., H. Kanamori, R. M. Allen, and E. Hauksson (2007). Determination of earthquake early warning parameters, τ_c and Pd, for southern California, *Geophys. J. Int.* **170**, 711–717.
- Zollo, A., G. Iannaccone, M. Lancieri, L. Cantore, V. Convertito, A. Emolo, G. Festa, F. Gallovic, M. Vassallo, C. Martino, et al. (2009). Earthquake early warning system in southern Italy: Methodologies and performance evaluation, *Geophys. Res. Lett.* **36**, L00B07, doi: [10.1029/2008GL036689](https://doi.org/10.1029/2008GL036689).

European Center for Geodynamics and Seismology
19 rue Josy Welter
7256 Walferdange, Luxembourg
jacek@ecgs.lu
(J.S., A.O.)

German Research Center for Geosciences
GFZ Potsdam
7 Helmholtzstrasse
14773 Potsdam, Germany
(D.B., M.P., S.P.)

Manuscript received 30 January 2015;
Published Online 25 August 2015